Influence of the cusp field on the plasma parameters of the Linac4 H^- ion source

S. Briefi[1,a)], S. Mattei[2], J. Lettry[2] and U. Fantz[1,3]

[1]*AG Experimentelle Plasmaphysik, Universität Augsburg, 86135 Augsburg, Germany*
[2]*Linac4 Ion Source Team, CERN-ABP, 1211 Geneva 23, Switzerland*
[3]*Max-Planck-Institut für Plasmaphysik, Boltzmannstraße 2, 85748 Garching, Germany*

[a)]Corresponding author: stefan.briefi@physik.uni-augsburg.de

Abstract. When the H^- ion source of CERN's Linac4 is operated in volume mode, a maximum of the extracted current is obtained at varying RF power. The power required for this maximum and its absolute value is strongly influenced by the cusp magnets installed at the source for electron confinement: without magnets, 15 – 20 mA are typically obtained at 20 kW whereas with magnets a factor of two more power is needed and 25 – 30 mA are achieved. In order to access the reasons behind the peaked performance with varying RF power and for determining the influence of the cusp field on the discharge, optical emission spectroscopy (OES) measurements of the atomic Balmer series and of the molecular Fulcher transition have been carried out. In all investigated cases, the gas temperature of the discharge has been virtually equal to the ambient temperature as the short discharge pulse length of 500 μs is not long enough for considerable heavy particle heating. When no cusp magnets are installed, the plasma parameters evaluated with the collisional radiative models Yacora H and Yacora H_2 show a minimum in the electron temperature of 3.25 eV and a maximum in the electron density of 4×10^{19} m^{-3} and also in the vibrational excitation of the hydrogen molecule at 20 kW. Assessing the relevant production and destruction processes demonstrates that the H^- yield is maximal at this point thereby explaining the optimum ion source performance. When the cusp magnets are applied, the same general trends are observed but the required RF power is a factor of two higher. The OES results indicate an optimum performance around 30 kW whereas the highest H^- current is actually achieved around 40 kW. Furthermore, a higher H^- yield is indicated without cusp magnets but a better ion source performance is observed with magnets. These differences can most likely be attributed to changing gradients in the plasma parameters which are not accessible by OES. Nevertheless, the obtained plasma parameters can be used as benchmark for RF coupling codes simulating the Linac4 ion source.

INTRODUCTION

Currently, an upgrade of the injector chain of the Large Hadron Collider (LHC) is realized at CERN which has the goal to improve both the particle beam brightness and the luminosity of the LHC. A crucial part of this upgrade is the construction of the Linac4 injector. It is foreseen as replacement for the ageing Linac2 which accelerates protons to 50 MeV before they are injected into the Proton Synchrotron Booster (PSB). In contrast, Linac4 is going to accelerate negative hydrogen ions up to 160 MeV and for the injection into the PSB the two electrons of the H^- ion are stripped with a thin foil [1]. The ion source of the Linac4 has to deliver an H^- current of 45 mA (for some special cases also up to 80 mA) in pulses of 500 μs at a repetition rate of 2 Hz. Negative hydrogen ions can be generated via two processes in general. The first method, the so-called volume process, relies on creating H^- in a plasma volume from vibrationally excited H_2 molecules. The second method, the so-called surface process, relies on the conversion of hydrogen atoms or ions on a surface with low work function [2]. In the latter case, caesium is evaporated into the ion source for establishing a low work function surface. Applying the surface process yields a higher H^- current but due to the high reactivity of caesium the work function of the surface and therefore the source performance degrades with time as caesium is removed and compounds are formed with the background gas. Therefore, sources operated in volume mode have the advantage of a higher temporal stability of the H^- current and reduced maintenance requirements.

At the Linac4 ion source cusp magnets are applied in order to reduce the losses of electrons to the discharge vessel wall. In general, for increasing the RF power also the extracted H^- current is increased up to one specific power level. Above this level the current decreases again. It has been observed that the cusp field has a strong influence

on the RF power required for the best source performance. With magnets, the highest current is achieved at 40 kW whereas without cusp the required RF power is reduced by a factor of 2 to 20 kW. In order to assess the reasons behind this behaviour, optical emission spectroscopy measurements (OES) of the molecular Fulcher-α transition and of the atomic Balmer series have been carried out at the Linac4 test stand. During these investigations the source has been operated in volume mode i. e. without adding caesium. The emissivities obtained from OES have been evaluated with the collisional radiative (CR) models Yacora H [3] and Yacora H_2 [4, 5] yielding discharge parameters like the electron density and temperature. This allows for the investigation of the influence of the changing plasma parameters on the relevant production and destruction processes taking place in the discharge volume and therefore on the H^- yield. Unfortunately, it has not been possible to extract a beam during the measurements due to hardware problems of the high voltage system, therefore a direct comparison between the determined plasma parameters and the beam properties could not be carried out. Typically, the maximum beam current with installed cusp magnets is around $25 - 30$ mA. Without magnets a reduced performance is obtained, only $15 - 20$ mA are usually extracted.

THE LINAC4 H^- ION SOURCE

Only a short description of the Linac4 ion source setup is given here, a more detailed one also including the extraction and beam formation system can be found in [6]. The plasma is generated via inductive RF coupling with a helical coil of four windings (see Figure 1 for a sketch of the plasma chamber). The RF amplifier operates at a frequency of 2 MHz with a maximum RF power P_{set} of 100 kW. The discharge pulse length is 500 μs with a repetition rate of 2 Hz. For the RF power values in this paper, the power delivered to the ion source P_{del} is always given, i. e. the power reflected due to a mismatch between the ion source impedance and the 50 Ω output of the generator is subtracted from the power set at the generator ($P_{del} = P_{set} - P_{refl}$). In order to reduce the loss of electrons to the ceramic plasma chamber wall, a Halbach-offset octupole cusp field is created by NdFeB permanent magnets. Hydrogen gas is supplied to the ion source with a fast piezo valve opening only for a short time prior to the RF pulse. The gas diffuses through the plasma chamber and is pumped through the extraction aperture. As the gas dynamics happens on the scale of several ten milliseconds [7] (whereas the RF pulse only lasts for 500 μs) the gas pressure can be treated as approximately constant during the RF pulse.

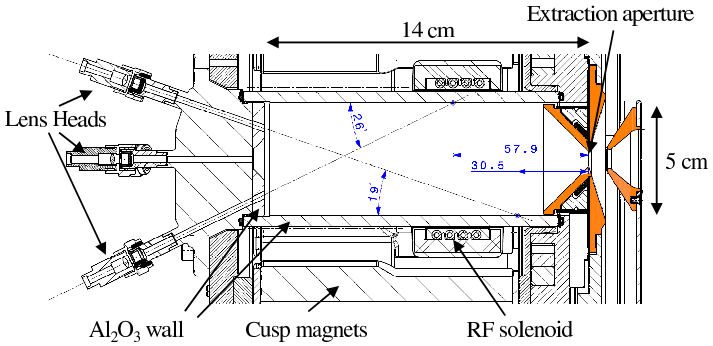

FIGURE 1. Sketch of the Linac4 ion source plasma chamber.

For optical emission spectroscopy measurements the discharge chamber can be accessed via three lens heads collecting the light emitted by the discharge. The lens heads are separated from the discharge by a sapphire window and focus the plasma emission into optical fibres leading to a spectrometer. The different lines-of-sight determined by the lens heads are tilted with respect to the central axis of the cylindrical discharge vessel: 0° which means on-axis, 19° and 26°. For the measurements presented in this paper only the on-axis view port has been used. The utilized high-resolution spectrometer (1 m focal length, grating 2400 grooves per mm) is equipped with an ICCD camera and has a Lorentzian apparatus profile with a full width at half maximum of 8 pm around 600 nm. For acquiring spectroscopic data, only the last 400 μs of the plasma pulse are considered to avoid recording the transient ignition phase. The intensity calibration of the system has been performed via an Ulbricht sphere serving as secondary radiation standard.

EVALUATING PLASMA PARAMETERS FROM OES

As already stated, the Balmer series of atomic hydrogen and the Fulcher transition of molecular hydrogen ($d\ ^3\Pi_u \rightarrow a\ ^3\Sigma_g^+$, located between 590 and 650 nm) were recorded by optical emission spectroscopy. For evaluating the obtained data the collisional radiative models Yacora H for atomic [3] and Yacora H_2 for molecular hydrogen [4, 5] are applied. These models calculate population densities via balancing all relevant population and depopulation processes for the particular states in the hydrogen atom or molecule, respectively. Processes including the reabsorption of photons have not been considered in order to facilitate the evaluation which means the plasma is treated as optically thin. As input parameters for the models the densities and temperatures of the neutral (H and H_2) and charged particles (electrons and H^+, H_2^+, H_3^+, H^-) are required. In order to determine plasma parameters from OES measurements, these input parameters are varied until both the absolute emissivities and the line intensity ratios of the measurements are matched thereby yielding the corresponding densities. However, for the investigated discharges, it turned out that the dominating population processes solely from atomic or molecular hydrogen and processes involving the hydrogen ions play only a very minor role. This eliminates the possibility of determining the densities of H^+, H_2^+, H_3^+ and H^- reliably. Besides the electron temperature and density only the densities of atomic and molecular hydrogen can therefore be obtained. It should be kept in mind that the intensities measured by OES represent line-of-sight averaged values, which means that also the determined plasma parameters have to be taken as line-of-sight averaged.

Another important input parameter for the CR models is the pressure of the hydrogen gas prior to the RF pulse as this determines the total number of particles available to the discharge. It is determined from the pressure in the plasma chamber via the ideal gas law. Due to the transient nature of the pulsed gas inlet, it is very difficult to give an exact number for the pressure within the plasma pulse and in-line pressure measurements are not possible due to the compact design of the ion source. Dedicated experiments concerning the gas particle propagation inside the vacuum setup of the ion source with respect to the gas valve settings have been carried out by replacing the discharge chamber with a T-shaped flange where a pressure gauge has been installed [7]. From these investigations, the gas pressure has been estimated to be at 3 Pa for the measurement campaigns presented in this paper.

Concerning the molecular Fulcher transition, the first twelve emission lines (rotational quantum numbers $N = 1, \ldots 12$) of the Q branch ($\Delta N = N' - N'' = 0$) arising from the first four diagonal vibrational transitions (vibrational quantum number $v' = v'' = 0, \ldots 3$) have been recorded. Figure 2 shows an exemplary emission spectrum of the corresponding wavelength range where the particular lines are labelled. From the measured emissivities the rotational population can be obtained. Typically, a non-Boltzmann rotational population is observed in hydrogen plasmas [8] which can be approximated by a two-temperature distribution [9]. The cold part of this distribution which is described by the temperature $T_{rot,1}$ reflects the population via heavy particle collisions. The hot part of the rotational population described by $T_{rot,2}$ is weighted relatively to the cold part by the factor γ for fitting. This part of the population can in general arise from recombinative desorption of hydrogen atoms at the wall of the discharge vessel, from dissociative recombination of H_3^+ with electrons, or from direct electron impact excitation [8]. For the discharge conditions present in the Linac4 ion source, the most likely process leading to the hot rotational distribution is collisional excitation by electrons. The gas temperature of the discharge can be determined by projecting $T_{rot,1}$ from the excited $d\ ^3\Pi_u$ state into the electronic ground state of the hydrogen molecule according to the rotational constants of the two states [10].

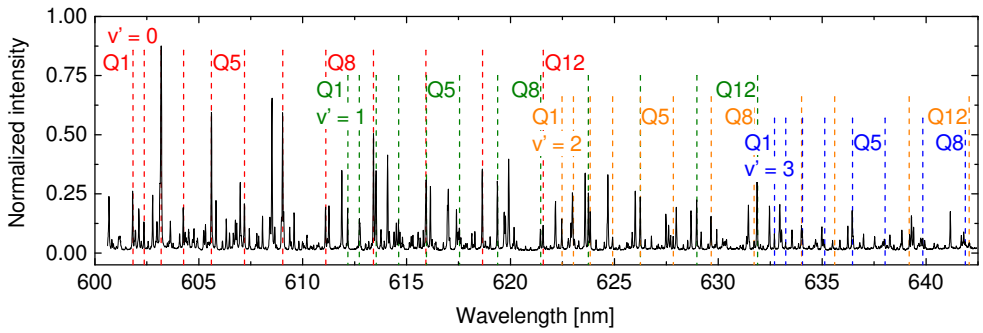

FIGURE 2. Example spectrum of the molecular Fulcher radiation. The drop lines indicate the position of the Q lines for the first four diagonal vibrational transitions.

RESULTS

Rotational population of H_2 and gas temperature

For evaluating the rotational distribution of the $d\ ^3\Pi_u, v' = 0$ state from the Fulcher emission, the measured emissivities of the rovibrational lines are divided by the statistical weight introduced due to the nuclear spin and by the Hönl London factors. When the logarithm of these values is plotted against the energy difference of the particular rotational levels, a Boltzmann distribution would in general lead to a linear slope. The left part of Figure 3 shows the rotational distribution obtained at an RF power of 40 kW. The two-temperature fit yields a value of $T_{rot,1} = 152$ K resulting in a gas temperature of $T_{gas} = 304$ K being virtually equivalent to the ambient temperature. Due to the low value of the cold rotational temperature, only the first rotational level and to a lesser extent also the second one follows the cold population. Therefore, one could argue if the high population in the $N = 1$ level is a statistical outlier and the actual gas temperature is much higher (in fact this was done for evaluating the first OES measurements [11]), but this is not the case: in the right part of Figure 3 the rotational population of the $d\ ^3\Pi_u, v' = 0$ state is shown operating the ion source exceptionally with deuterium. The non-Boltzmann character of the distribution is also clearly present for D_2 and similar to H_2 a value of $T_{rot,1} = 155$ K is obtained. Due to the higher mass of D_2 the energy difference between the particular rotational levels is smaller. This leads to a higher number of levels following the cold distribution making it much more evident compared to hydrogen. The cold gas temperature can be explained by the short discharge duration of only 500 μs which prevents the heavy particles from heating up considerably. For all investigations, the gas temperature of the discharge has always been virtually equivalent to the ambient temperature and no influence of RF power or the cusp magnets could be determined.

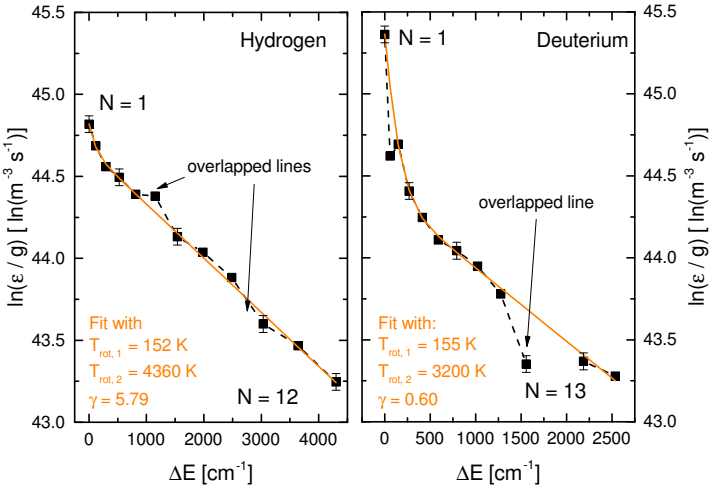

FIGURE 3. Rotational distribution within the $d\ ^3\Pi_u, v' = 0$ state evaluated from the Fulcher emission recorded for an RF power of 40 kW in deuterium and hydrogen. The corresponding two-temperature fits are also plotted.

RF power variation without cusp field

When no cusp magnets are installed at the ion source, its operational range with respect to the RF power is limited to 5 – 40 kW, otherwise either the discharge ignition or its stable operation is not possible. Figure 4 shows the emissivities measured for varying the RF power in this range (the RF power required for best performance is indicated by the grey hatched area around 20 kW). It can be seen that the atomic Balmer radiation steadily increases with increasing RF power whereas the molecular Fulcher radiation shows a minimum between 10 and 20 kW. The electron temperatures and densities obtained from evaluating the CR models are summarized in Figure 5. The value of T_e decreases from 3.75 to 3.25 eV when the power is increased from 5 to 15 kW. Above 15 kW, T_e increases again reaching values of 3.90 eV at 40 kW. The electron density shows a contrary behaviour, increasing from 1.6×10^{19} m^{-3} at 5 kW to a peak value of 4×10^{19} m^{-3} achieved between 15 and 25 kW. The density ratio of atomic to molecular hydrogen obtained

from the OES measurements is shown in Figure 6. For increasing RF power, the density ratio increases steadily from 0.28 at 5 kW to a value of around 0.6 above 25 kW.

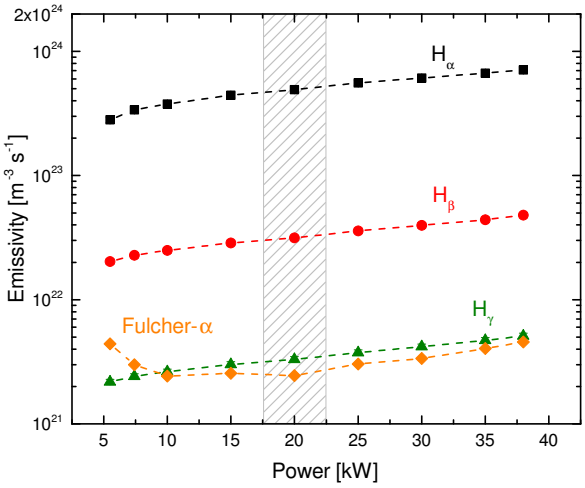

FIGURE 4. Emissivities of the atomic Balmer and of the molecular Fulcher radiation at varying RF power without applying a magnetic cusp field. The grey hatched area shows the region where the optimum source performance is typically achieved.

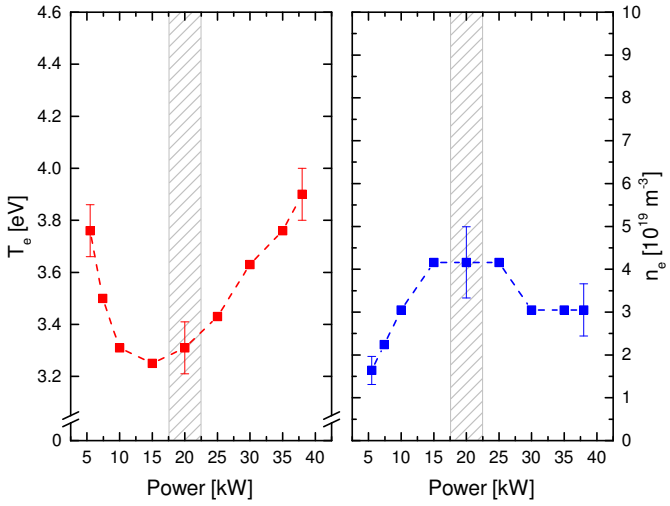

FIGURE 5. Electron temperature T_e and electron density n_e evaluated from the OES measurements for varying RF power without applying a magnetic cusp field. The grey hatched area shows the region where the optimum source performance is typically achieved.

For such plasma parameters, the dominating destruction process for negative hydrogen ions is collisional detachment by electrons: $H^- + e_{fast} \rightarrow H + 2e$. Balancing this destruction process with the formation process $H_2(v) + e_{slow} \rightarrow H^- + H$ shows that the electron density does not influence the H^- yield as both reaction rates depend linearly on n_e. Concerning the electron temperature, a low value of T_e is highly beneficial for the H^- yield as the production rate increases with lower electron energy and also the destruction rate decreases. Furthermore, the vibrational excitation of the electronic ground state of hydrogen influences the production rate considerably as the formation process is more efficient the higher the vibrational excitation. A variety of processes such as cascades from higher lying electronic states or reformation of hydrogen atoms where parts of the binding energy is converted into vibrational excitation contribute to the vibrational population. Many of those processes happen on time scales being larger than the discharge pulse length of 500 μs leading to the fact that the vibrational distribution is far off from

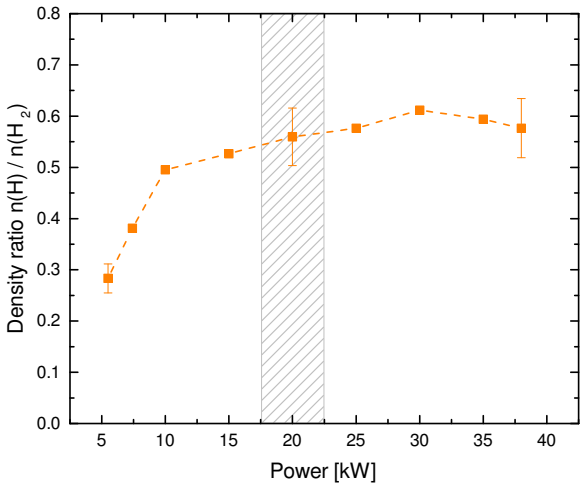

FIGURE 6. Density ratio of atomic to molecular hydrogen obtained from the OES measurements for varying RF power without applying a magnetic cusp field. The grey hatched area shows the region where the optimum source performance is typically achieved.

equilibrium in the ion source plasma. Nevertheless, the vibrational population of the first four levels ($v' = 0, \ldots 3$) is accessible via summing up over the rotational population measured in each vibrational state. In doing so, a vibrational temperature can be determined and a maximum of this temperature is obtained at an RF power of 20 kW. Concerning the density ratio of atomic to molecular hydrogen, a higher value is in general adhere to a large H^- production rate as there are less molecules available. However, for low RF powers where $n(H)/n(H_2)$ is low, the vibrational temperature is low and the electron temperature is high. In summary these considerations can explain that the best performance of the ion source is achieved at 20 kW as a low electron temperature and a high vibrational excitation is obtained.

RF power variation with cusp field

The operational range of the ion source is shifted to higher values when the cusp magnets are installed: instead of 5 – 40 kW without cusp, the RF power can be varied between 10 and 70 kW. This behaviour arises from the fact that the cusp field is designed in a way that prevents the electrons from getting close to the wall of the discharge vessel where the heating RF field is most intense. As the over-all heating capability is therefore reduced, the RF power demand is higher when the cusp magnets are installed in the ion source.

Figure 7 shows the emissivities measured with cusp field. As already stated, the best ion source performance is achieved around 40 kW which is a factor of two higher than without magnets. The general trends of the emissivities are the same as observed without cusp magnets: the emissivity of the atomic Balmer lines increases steadily with power whereas the molecular Fulcher emission shows a minimum, lying now between 15 and 30 kW. Furthermore, the absolute intensities are higher with cusp magnets.

During the comparison of the general plasma parameter trends, it turned out that the behaviour is very similar for installed cusp magnets or removed ones. However, the higher power demand with cusp magnets is also mirrored in the plasma parameters: for similar discharge conditions the required RF power is around a factor of two higher than without magnets. Figure 8 show the electron temperature and density obtained with cusp. For comparison, the values determined without cusp field are also included, an additional x-axis in blue colour has been introduced at the top of the graph (this axis is scaled by a factor of two compared to the x-axis at the bottom of the graph). It can clearly be seen that the same general trends are observed for T_e and n_e with and without cusp magnets: a minimum in the electron temperature and a maximum in the electron density for varying RF power. With cusp field, higher absolute values of T_e and n_e are obtained and the position of the extremes is slightly shifted from the point of optimum source performance to lower RF powers. The same is true for the vibrational temperature reaching a maximum at 30 kW. Concerning the density ratio of atomic to molecular hydrogen (see Figure 9), not only the same general trend is observed but also comparable absolute values over the whole RF power range are obtained for both cases.

Therefore, the optimum source performance would be expected at an RF power of 30 kW as the electron temper-

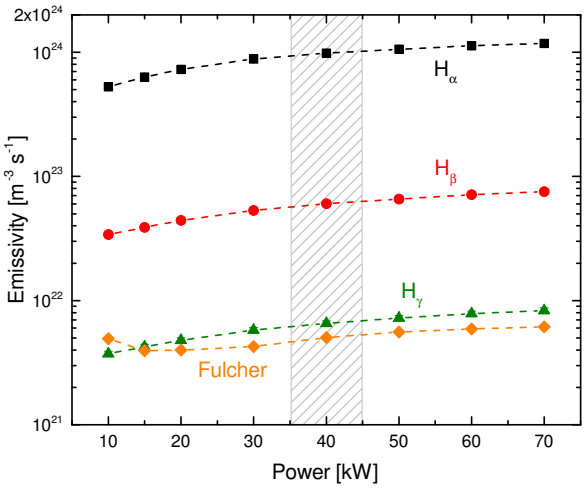

FIGURE 7. Emissivities of the atomic Balmer series and the molecular Fulcher transition for varying RF power with applying a magnetic cusp field. The grey hatched area shows the region where the optimum source performance is typically achieved.

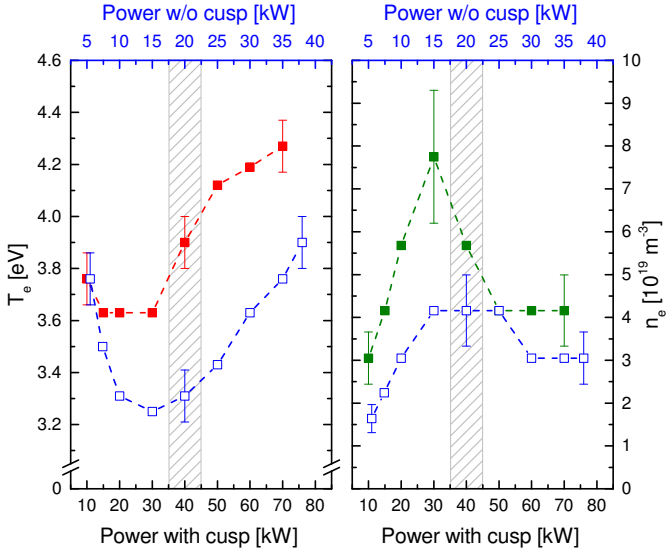

FIGURE 8. T_e and n_e obtained from the OES evaluation for varying RF power and with applying a magnetic cusp field (full symbols). The open symbols reflect the results obtained without cusp field and belong to the upper x-axis. The grey hatched area shows the region where the optimum source performance is typically achieved with and without cusp magnets.

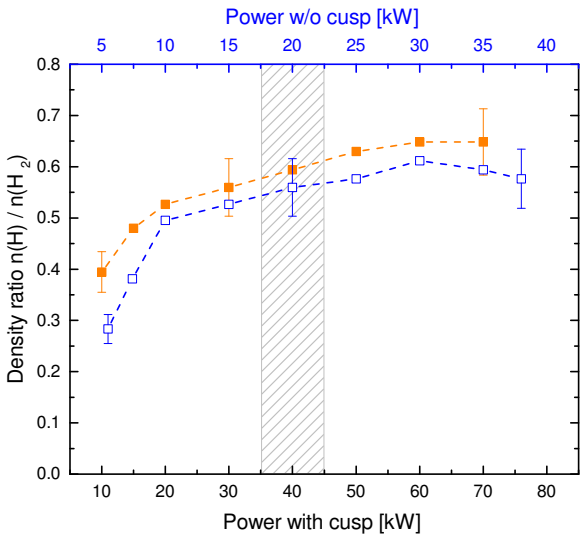

FIGURE 9. Density ratio of atomic to molecular hydrogen obtained from the OES evaluation for varying RF power and with applying a magnetic cusp field (full symbols). The open symbols reflect the results obtained without cusp field and belong to the upper x-axis. The grey hatched area shows the region where the optimum source performance is typically achieved with and without cusp magnets.

ature has its lowest value there and the vibrational excitation is highest. However, the highest H^- current is achieved at 40 kW of RF power. Furthermore, the absolute value of T_e is lower without cusp magnets what should result in a higher H^- yield, but the ion source performance is better with magnets. In order to assess the reasons for these differences in expected and observed performance, it should be kept in mind that a rather large plasma volume is probed by OES due to the inherent line-of-sight integration whereas the H^- ions are actually extracted from only a small region close to the extraction aperture. In addition, different plasma parameter profiles (which will especially be present when comparing the plasma with and without cusp field) cannot be assessed and considered in the OES evaluations. Such spatial variations of the plasma need to be considered in order to explain the performance differences with and without cusp field.

SUMMARY AND CONCLUSION

In order to assess the different performance of the Linac4 H^- ion source with respect to the application of cusp field magnets, optical emission spectroscopy measurements have been carried out while operating the ion source in volume mode. Typically, the extracted H^- current shows a maximum at varying RF power of 15 – 20 mA at 20 kW without cusp magnets and of 25 – 30 mA at 40 kW with cusp field. In both cases, the electron temperature shows an initial decrease with RF power before it rises again whereas the electron density shows a contrary peaking behaviour. An assessment of the relevant production and destruction processes of H^- predicted a maximum H^- yield at 20 kW which is exactly the value where the best ion source performance is achieved.

When the cusp magnets are applied, their field topology prevent the electrons from getting close to the wall of the discharge vessel where the intense RF fields are located. Therefore, a higher RF power is required to reach similar discharge parameters as without cusp field. This can be seen in all determined parameters, as the observed general trends for varying RF powers are shifted by a factor of two to higher powers when the cusp magnets are installed. Considering the H^- yield, the predicted RF power for best performance is at 30 kW whereas the highest current is actually achieved at 40 kW. Furthermore, a higher H^- yield is expected when the cusp magnets are not installed, but the contrary behaviour is observed. These differences can most likely be attributed to changes in the plasma parameter profiles which cannot be accessed by optical emission spectroscopy. Nevertheless, the obtained plasma parameters can be used as benchmark values for RF coupling codes simulating the Linac4 ion source [12–14].

ACKNOWLEDGMENTS

The authors would like to thank the Deutsche Forschungsgemeinschaft (DFG) for their support within the project BR 4904/1-1.

This work has been carried out within the framework of the EUROfusion Consortium and has received funding from the Euratom research and training programme 2014-2018 under grant agreement No 633053. The views and opinions expressed herein do not necessarily reflect those of the European Commission.

REFERENCES

[1] L. Arnaudon *et al.*, "Linac4 technical design report," (2006), CERN-AB-2006-084 ABP/RF.
[2] M. Bacal and M. Wada, Appl. Phys. Rev. **2**, p. 021305 (2015).
[3] D. Wünderlich, S. Dietrich, and U. Fantz, J. Quant. Spectr. Rad. Transfer **110**, 62 – 71 (2009).
[4] D. Wünderlich, Ph.D. thesis, University of Augsburg (2004).
[5] D. Wünderlich and the NNBI Team, Proceedings of the 30th ICPIG, Belfast, Northern-Ireland (2011).
[6] J. Lettry *et al.*, AIP Conf. Proc. **1515**, 302–311 (2013).
[7] E. Mahner *et al.*, AIP Conf. Proc. **1515**, 425–432 (2013).
[8] P. Vankan, D. Schram, and R. Engeln, Chem. Phys. Lett. **400**, 196 – 200 (2004).
[9] S. Briefi, D. Rauner, and U. Fantz, submitted to J. Quant. Spectr. Rad. Transfer, 2016.
[10] S. A. Astashkevich *et al.*, J. Quant. Spectrosc. Radiat. Transfer **56**, 725 – 751 (1996).
[11] S. Briefi *et al.*, Rev. Sci. Instrum. **87**, p. 02B104 (2016).
[12] S. Mattei *et al.*, AIP Conf. Proc. **1515**, 386–393 (2013).
[13] T. Shibata, S. Mattei, K. Nishida, J. Lettry, and A. Hatayama, AIP Conf. Proc. **1655**, p. 020008 (2015).
[14] S. Mochizuki *et al.*, AIP Conf. Proc. **1655**, p. 020016 (2015).